Determination of petrophysical properties of Sadi Formation in Halfaya oil field, southern Iraq

Mustafa M. Hashim [a, b], **Ghanim M. Farman** [a, *], **Ahmed Askar** [c]

a Department of Petroleum Engineering, College of Engineering, University of Baghdad, Iraq
b Department of Petroleum Engineering, College of Engineering, University of Kerbala, Iraq
c Geophysics Department, Collage of Remote Sensing and Geophysics, Al–Karkh University for Science, Iraq

Abstract

This study aimed to evaluate the reservoir petrophysical properties (porosity, water saturation, and permeability) for optimal flow unit assessment within the Sadi Formation. Utilizing open hole logging data from five wells, the Sadi formation was divided into two rock units. The upper unit (A) is 45-50 meters thick, mainly consisting of limestone, mainly consisting of shaly limestone at the lower part. The lower unit (B) has a thickness of approximately 75-80 meters and is primarily composed of limestone, further subdivided into three subunits (B1, B2, B3). The average water resistivity is 0.04 ohm-m, and the average mud filtrate resistivity is 0.06 ohm-m. The Pickett plot was utilized to determine Archie parameters (tortuosity factor=1, cementation factor= 2, saturation exponent = 1.94). Petrophysical properties were determined through a sequence of operations involving lithology identification, shale volume estimation, porosity calculation, water saturation calculation, and permeability estimation. Lithology was identified using neutron, density and sonic logs with (N-D, M-N) cross plots, which show that the Sadi Formation is mainly limestone. The Gamma ray log was employed to estimate the shale volume of the Sadi Formation using the Larionov equation of old rock, resulting in a shale volume of 7%-58%. After calculating porosity using neutron-density logs, the resulting porosity matched the core porosity. Archie equation was used to calculate the formation's water saturation, with water saturation less than 0.48 (cut-off) obtained in B1, B2 and B3 units. Finally, the formation permeability was estimated using the Flow Zone Indicator method, which provided a good match with core permeability. Porosity and water saturation were estimated with depth using Techlog software. The best hydrocarbon-holding unit is B2, which has the highest porosity, lowest water saturation, and the best permeability, with a thickness of 20.1 meters. As a result of this study, core plug analysis and well logging data identified eight distinct units in the Sadi Formation. There are three flow sub-units in upper Sadi (B1), three flow sub-units in Sadi (B2) and two sub-units in Sadi (B3). Additionally, it has been found that the marl rock unit (A2) separates the water-bearing zone (A1) from the oil-bearing zone (B).

Keywords: Sadi Formation; Halfaya Oil Field; Petrophysical Properties.

1- Introduction

For petroleum geologists, well logging provides detailed records for various geological rock units penetrated by oil wells. Well-logging, based on physical measurements, is used to characterize lithology, pore geometry, and porosity, as well as to determine permeability [1].

The basics of well logs interpretation also involve measuring true resistivity of the field, total porosity, mud filtrate resistivity, water salinity, effective porosity, and water saturation. These parameters help compute the overall reserves and evaluate the commercial viability of hydrocarbon deposits. Engineers can enhance the available records to assist in calculating initial oil in place OOIP [2].

Data can be collected from two sources when dealing with these properties: instrumental techniques that evaluated the properties versus depth, known as logs, and the real samples that practically reflect the formation, such as core samples [3]. Cross plots are commonly used to demonstrate the influence of pairs of logs responding to porosity and lithology, providing a graphic representation of different mixes [4]. Quantitative assessment of hydrocarbon accumulation in a reservoir requires an accurate prediction of clay volume, which can block pore space, decrease total permeability, and consequently affect reservoir quality [5]. Various well logs may be used to assess porosity indirectly by utilizing multiple elements that indicate characteristics of the formation and the fluid within [6]. One of the key tasks is calculating water saturation, which affects fluid distribution in the reservoir and makes hydrocarbon estimations more challenging than porosity due to the degree of uncertainty involved and the number of measurements needed [7]. For reservoir engineers, permeability is a fundamental component and a crucial factor in managing the reservoir development, such as selecting the most optimal production rate for wells and designing water injection

schedules [8]. The reservoir was divided into zones using a hydraulic flow unit, with each flow unit recognized by employing a flow zone indicator (FZI), which is also used to compute permeability in situations where core data is unavailable [9]. The Sadi Formation is a productive and promising giant reservoir that contains some clay and marl intervals [10]. Well log data from five oil wells were utilized in this research to investigate these topics. We have ascertained critical characteristics, including Archie's parameters, mud filtrate resistivity, and formation water resistivity, through advanced analysis and adjustments for environmental conditions. Petrophysical characteristics, such as porosity, permeability, water saturation, and net-to-gross ratio, can be emphasized using these data and are essential for maximizing hydrocarbon production from the Sadi Formation. While previous studies determined the general flow unit of the Sadi Formation (zonation), the current study identifies the most efficient flow unit within the formation, leading to better decision-making, such as selecting the most profitable unit for horizontal drilling. This study provides important new information and deepens our knowledge of carbonate reservoirs, paving the way for more efficient oilfield development and management.

2- Geological setting

The Halfaya oil field is located in Missan province, approximately 35 km southeast of Amara City. The field spans 38 km in length and 12 km in width, featuring a NW-SE trending anticline structure. It belongs to the Tigris sub-tectonic Formation of the Mesopotamian basin. The rise and fall of the sea level, resulting from the tectonic movements in the area during the late Cretaceous, led to multiple cycles of deposition in Sadi-B3, creating a diversity of inner ramp microfacies. While middle ramp facies developed in Sadi-B2 Formations, outer ramp facies developed in the uppermost of Sadi-B1 and Sadi-A Formations, representing a transition from ramp to basinal conditions. In 1976, the Sadi reservoir was discovered within the Halfaya oil field in Iraq. The Late Cretaceous Sadi Formation overlies the Tanuma Formation with a conformable contact at the top of the black calcareous shale and the base of the white and chalky limestone. It underlies the Hartha Formation with erosional unconformity contact. The average formation thickness of the Sadi formation is between 120 and 130 meters.

3- Materials and methods

Petrophysical characteristics were analyzed using open-hole logs in five wells of the Sadi Formation at the Halfaya field. While certain logs are accessible in image format, which cannot be loaded directly into Schlumberger Techlog software, the majority of logs are available in digital format (LAS). To convert these logs into LAS files, digitization was performed using Neuralog (version 2015.04). Additionally, well HF005 provides

core plugs with porosity-permeability values. Quality control was implemented in two stages for all logging measurements, as the accuracy of the results depends on the quality of the input. Firstly, using the gamma-ray as a reference log, the depth of every log in each well was inspected for matching reasons. Furthermore, environmental correction was applied to eliminate the impact of the borehole condition on logs that the supplier. As shown in Fig. 1, the procedures used in this research are divided into five sections.
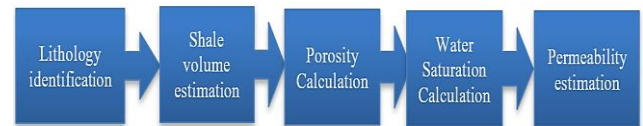
Fig. 1. Research procedure

3.1. Lithology Identification

Cross plots are graphical representations that illustrate the relationship between the direction and intersection of two logs, which are influenced by the properties of pore fluid and matrix lithology. This deposit may possess a pore structure with varying porosity due to its mix of rock and fluid [11]. In this investigation, mineral identification (M-N) and matrix identification (N-D) cross plots were used. These cross plots were computed using the equations provided by Dewan [12] and are shown in Fig. 2 and Fig. 3. M-N parameters calculated with Eq. 1 and Eq. 2:

$$M = (\Delta t_f - \Delta t_{log}) / (\rho_b - \rho_f) \times 0.01 \qquad (1)$$

$$N = (\text{Ø}N_f - \text{Ø}N) / (\rho_b - \rho_f) \qquad (2)$$

Where: Δt_f = interval transit time for fresh water =189 m/s and 185 m/s for salt mud. Δt = sonic log reading. ρ_b = density log reading. ρ_f= density of fresh water = 1 g/cm3 or 1.1 g/cm3 for salt mud. $\text{Ø}N_f$ = Porosity of Neutrons for Fluid =1. $\text{Ø}N$ = neutron porosity.
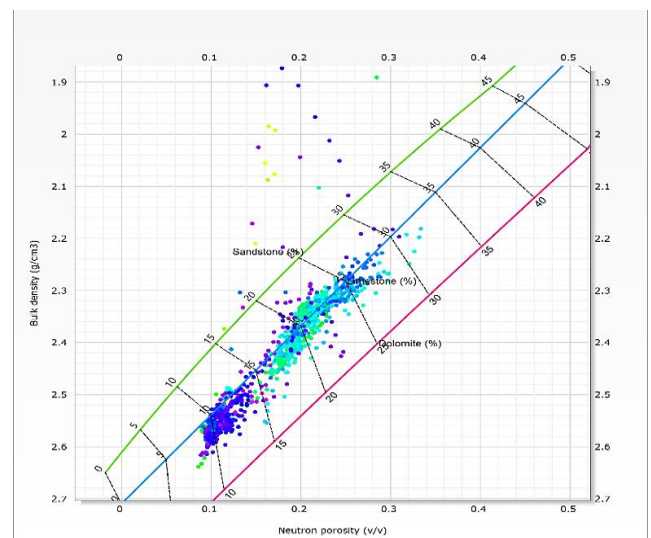
Fig. 2. N-D cross plot of well HF005-M316
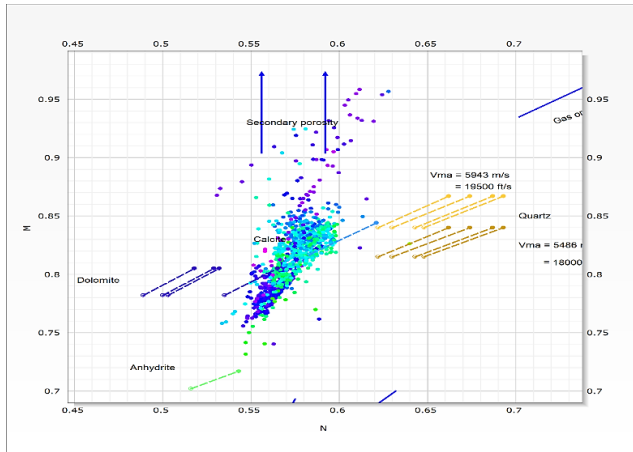
Fig. 3. M-N cross plot of well HF005-M316

3.2. Shale volume estimation

In petrophysical formation evaluations, calculation the volume of shale or the rock portion that is involved of clay minerals is a very essential step [13]. Shale has a crucial role in determining the existence of hydrocarbons [14]. The volume of shale is calculated in the Sadi Formation using gamma-ray measurements, according to the Eq. 3:

$$IGR = \frac{GR_{log} - GR_{min}}{GR_{max} - GR_{min}} \tag{3}$$

Subsequently, use an empirical Eq. 4 designed for old rocks to transform the gamma-ray index into shale content, the resulted shale shown in Fig. 4.

$$Vsh(old\ rock) = 0.33 \times (2^{2 \times IGR} - 1) \tag{4}$$

Where: IGR: gamma-ray index, GR log: gamma-ray log reading in the zone of interest, API units, GR min: minimum gamma-ray reading in a clean zone, API units, GR max: maximum gamma-ray reading in shale zone, API units.
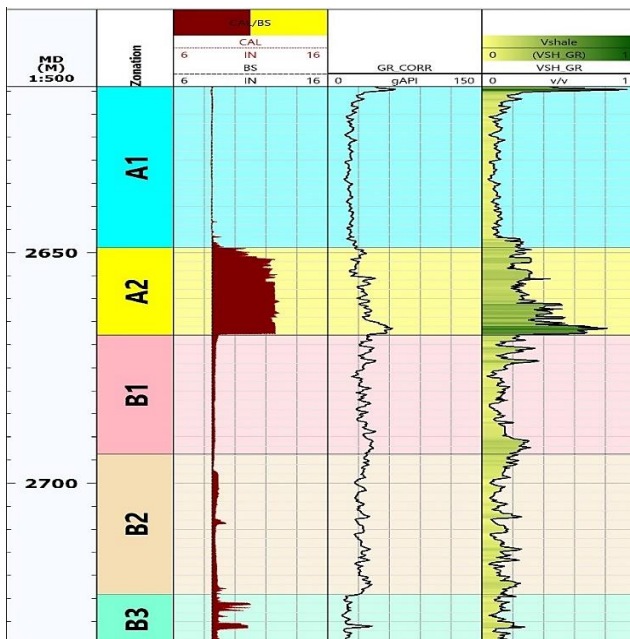
Fig. 4. Shale volume of HF005-M316

3.3. Porosity calculation

Porosity is a crucial property because it represents Hydrocarbon storage space. In addition, other petrophysical properties, such as saturation and permeability, are influenced by the connected pores [15]. Porosity is calculated by dividing the volume of pores by the total volume of the matrix according to Eq. 5.

$$porosity = \frac{pore\ volume}{total\ volume} \tag{5}$$

Engineers compute porosity as a fraction. Geologists often utilize a percent to represent porosity, which is calculated by multiplying the porosity value by 100. Porosity effective which are "connected" pores are porosity that allows fluid movement. Porosity is a scalar parameter since it is the total volume to estimate the size of the sample. Visual approaches and lab testing are employed to measure porosity for cases in testing, the more evident of pores. Porosity is typically determined during reduced microscopic inspection of core plugs. In 1952, Archie category gives a technique for estimating total porosity depending on visual and texture parameters. Visual porosity may be measured by thin-section estimates or image-analyzing algorithms to quantify pore space from thin-section images[16, 17]. Without point counts, visual estimations may be incorrect[18, 19]. Visual estimations of pore space from thin-section pictures compared to point counts may be less precise, which are regarded the best standard for estimating porosity[20]. The porosity of the rocks may be assessed utilizing neutron, sonic, and formation density. The mineralogy, pore fluid composition, and shale content of the rock are additional factors, alongside porosity, that can affect well logs readings. Assessing porosity often relies on merging logs as an interdependent method. The results of these tools are significantly impacted by properties of the formation adjacent to the borehole. While the sonic log is not the most suitable tool for deep investigation, neutron and density logs often reveal considerable variation within the invaded zone. However, the specific depth at which this occurs depends on the porosity [21, 22].

- Effective porosity

As Dodge et al. explain, engineers typically use the term 'effective porosity' to describe the interconnected pores within a rock. Effective porosity is calculated as the total porosity minus the water bounded to clay minerals within the rock [23]. The resulted porosity of Eq. 6 is compared with core porosity in Fig. 5.

$$\emptyset_{eff} = \emptyset_t \times (1 - Vsh) \tag{6}$$

Where: $\emptyset_{eff}$: effective porosity. $\emptyset_t$: total porosity.

3.4. Water saturation calculation

Water saturation (Sw) represents the ratio of water-filled pore space to the total pore volume in the rock.

Hydrocarbon saturation(Sh) refers to the portion of pore space that is not filled with water [24]. The relationship between the two is expressed as:

$$Sw + Sh = 1 \qquad (7)$$

Where: Sw: Water saturation. SH: Hydrocarbon saturation.
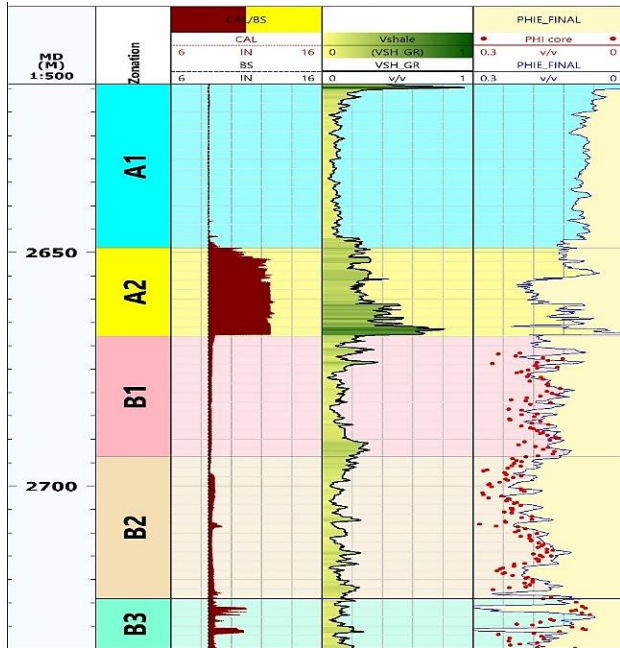
Fig. 5. Effective porosity of HF005-M316

Water saturation is a crucial parameter in well logs interpretation as it indicates the percentage of water volume relative to the pore volume. The primary objective of well logging is to evaluate water saturation and determine hydrocarbon saturation. [25].

Archie's equation is a key tool for predicting water saturation based on resistivity log in formations, whether heterogeneous or clean homogeneous formations. Its original formulation has proven to deliver reliable results [26, 27].

$$Sw^n = \frac{\emptyset}{\emptyset^m} \times \frac{R_w}{R_t} \qquad (8)$$

Where: a: is the tortuosity factor. m: is the cementation factor. n: is saturation exponent. Sw: the water saturation. Rw: is the resistivity of the formation (connate) water. Rt: is the true resistivity of the formation ohm.m.

The accuracy of the Archie equation depends on the precision of its fundamental input parameters: Rt, Rw, and Ø. Thus, the key issue in reliably determining water saturation from resistivity logs is selecting adequate values for Archie's parameters (a, m, and n), which vary based on rock lithology and porosity[28, 29]. The parameters (a, m and n) are typically determined using the Pickett plot. Fig. 6 demonstrates a good correlation between water saturation obtained from the Archie equation and core-measured saturation**.**
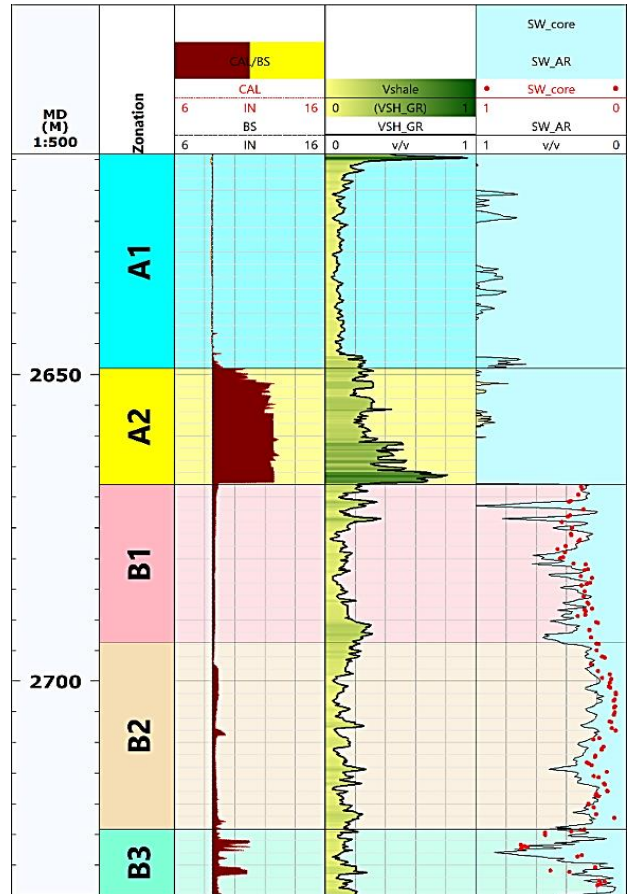
Fig. 6. Water saturation of HF005-M316

3.5. Permeability estimation

Amaefule et al. demonstrated that permeability can be estimated using a flow zone indicator (FZI) [9]. The FZI is a distinct parameter for every hydraulic flow unit, obtained from the intercept at a normalized porosity index (Øz) of 1 on the unit slope line, as shown in Fig. 7. This line is generated by plotting the reservoir quality index (RQI) against the normalized porosity index (Øz), using the following equations:

$$RQI = 0.0314 \times \sqrt{\left(\frac{k}{\emptyset}\right)} \qquad (9)$$

$$\emptyset z = \frac{\emptyset}{1-\emptyset} \qquad (10)$$

$$FZI = \frac{RQI}{\emptyset z} \qquad (11)$$

To estimate permeability for each flow unit in the formation, a unique equation for each distinct flow unit can be derived by plotting core permeability versus core porosity, as shown in Fig. 8. Table 1 provides the equations for each unit used to estimate permeability.

As illustrated in Fig. 9, permeability values estimated using the FZI method show a strong agreement with core permeability measurements.

Table 1. Flow zone indicator permeability formula for Sadi Formation

HFU	Reservoir quality	Equation	R^2
HFU-1	very good quality	$k = (1014*(0.8231^2)*(Ø^3))/(1-Ø)^2$	0.96
HFU-2	moderate quality	$k = (1014*(0.3167^2)*(Ø^3))/(1-Ø)^2$	0.94
HFU-3	Fair rate quality	$k = (1014*(0.1648^2)*(Ø^3))/(1-Ø)^2$	0.84
HFU-4	poor quality	$k = (1014*(0.0823^2)*(Ø^3))/(1-Ø)^2$	0.77
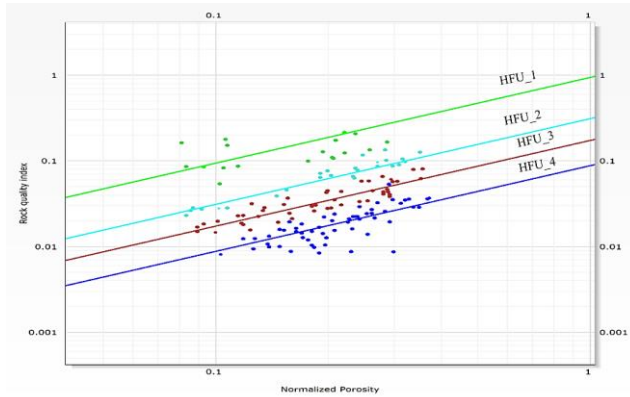
Fig. 7. Rock quality index vs Normalized porosity cross plot for Sadi Formation
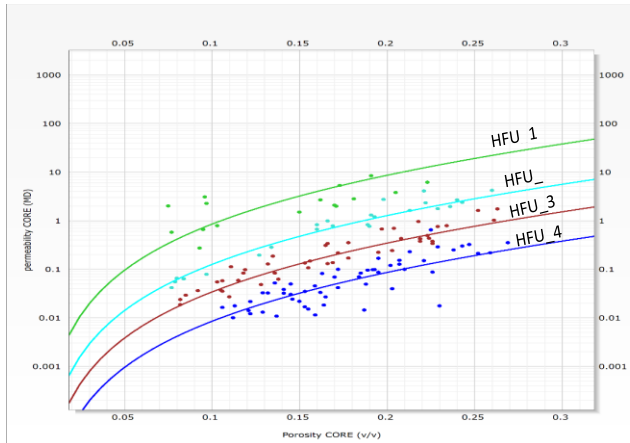
Fig. 8. Core permeability vs core porosity cross plot for FZI method of Sadi Formation
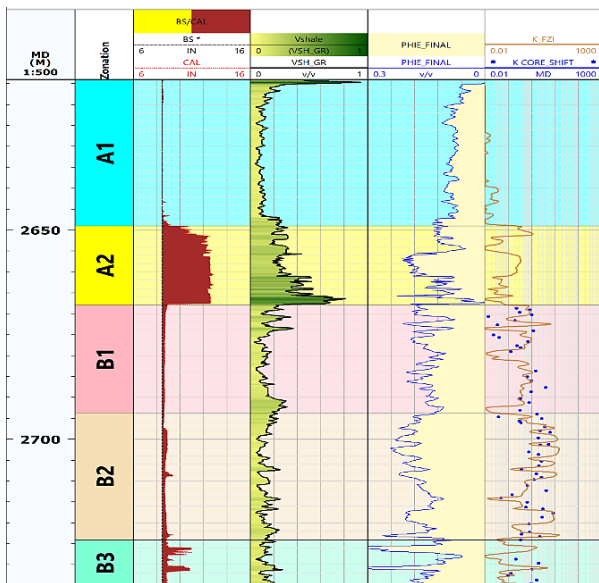
Fig. 9. Permeability with Flow Zone Indicator method and core permeability of well HF005-M316

4- Results

4.1. Cut-off calculations

In petroleum engineering, cut-offs refer to the thresholds at which the fluid flow processes are stopped.

- Porosity Cut-off

Sections of rock are excluded due to poor porosity and low permeability, rendering them non-productive. The typical porosity threshold for sandstones is around (8-10) %, whereas for limestones, it ranges from 3-5 %. The lower porosity cut-off in limestone indicates its tendency to exhibit significant fracturing. [30].
For the Sadi Formation, the porosity cut-off was determined by analyzing a permeability-porosity cross-plot. A typical permeability cut-off equal to 0.1 MD was applied, leading to an identified porosity cut-off of around 0.08, as shown in Fig. 10 (a).

- Water Saturation Cut-off

The water saturation cut-off is established by correlating the porosity log with water saturation values from the studied wells. This involves identifying the porosity log cut-off and locating its intersection on the curve to determine the water saturation cut-off. For the Sadi Formation, the water saturation cut-off was found to be 0.48, as shown in Fig. 10(b).

4.2. Net to gross (N/G)

Net pay indicates the thickness of the commercially feasible permeable and porous zone containing significant hydrocarbons. The net pay-to-gross pay ratio is a critical metric estimating reservoir volume, defining the relationship between net and gross compensation. Once the cut-off values for the porosity log and water saturation are determined, the net pay thickness to gross thickness can be calculated by excluding sections with water saturation values exceeding the cut-off and porosity values below the cut-off. [31]. The following formula is used to determine the net-to-gross ratio (NTG) for each well:
NTG = Net Pay thickness of Reservoir/ Gross Thickness of Reservoir
Where: reservoir net pay thickness is the total thickness of the pay with porosity greater than the cut-off percentage and water saturation below than the cut-off value. Whereas reservoir gross depth is the entire thickness of the reservoir.
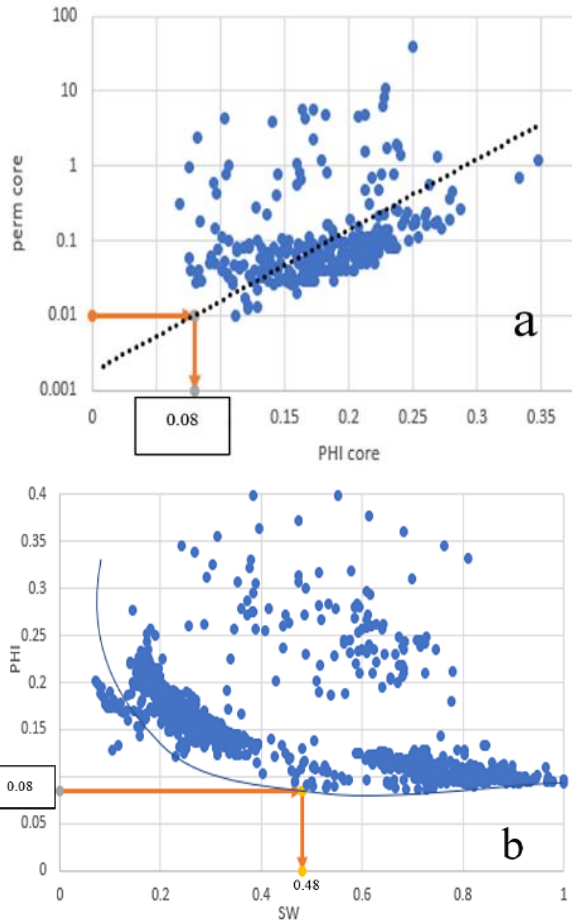
Fig. 10. Halfaya oil field cut-off (a) porosity cut-off, (b) water saturation cut-off

The average net pay within the contract area is 13.9 m for Sadi B1, 20.1m for Sadi B2 and 7.7m for Sadi B3. The B2 unit in the Halfaya oil field exhibits the best pay zones, as shown in Fig. 11 and Fig. 12.
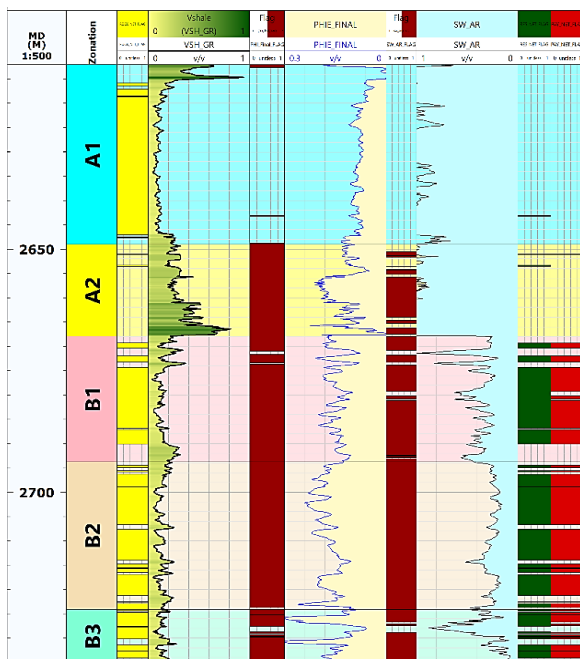
Fig. 11. Net to Gross of HF005-M316
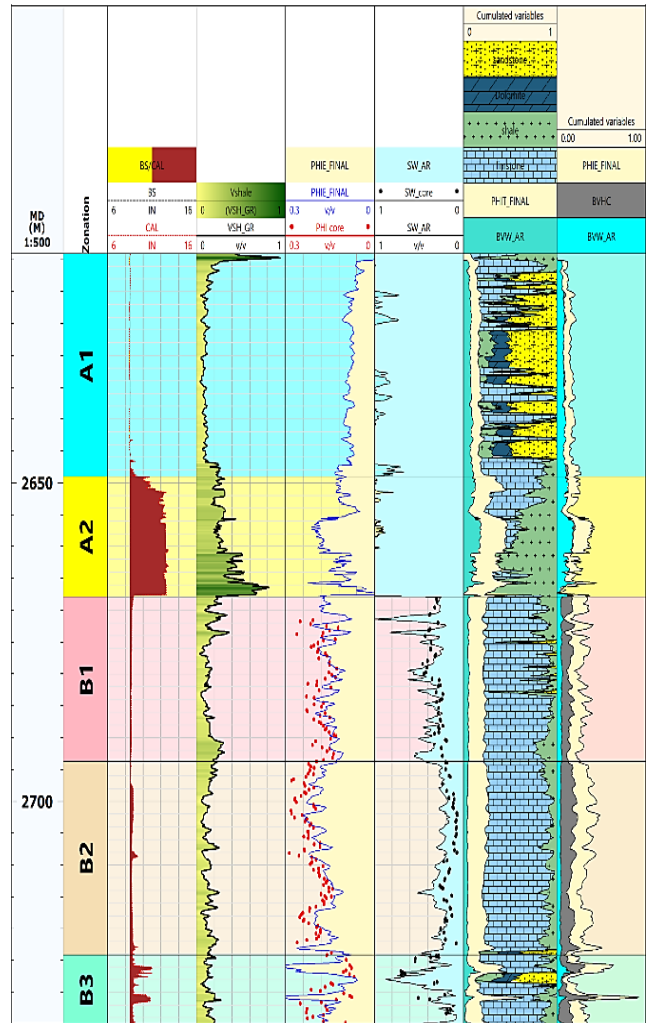
Fig. 12. Computer processing of HF005-M316

4.3. Flow unit identification

To identify flow units, data from well logs and cores must be collected. This includes information on pore throats sizes, petrophysical characteristics, and rock types. Such data enables the calculation of curves (φ, Sw, k) derived from core measurements and conventional electric logs. These calculations are essential for estimating flow units using petrophysical parameters [27]. High-quality input data ensures more dependable outputs, facilitating the development of a more accurate reservoir characterization. One of the techniques concerned in determining the flow units is:

- Well log interpretations

This technique involves analyzing the variation of water saturation with formation depth, as well as plotting water saturation against porosity. The resulting curves are shown in Fig. 13. According to Hartmann and MacMillan, a decrease in porosity typically leads to an increase in water saturation. The variations in Sw and φ values highlight distinct pore types [19].
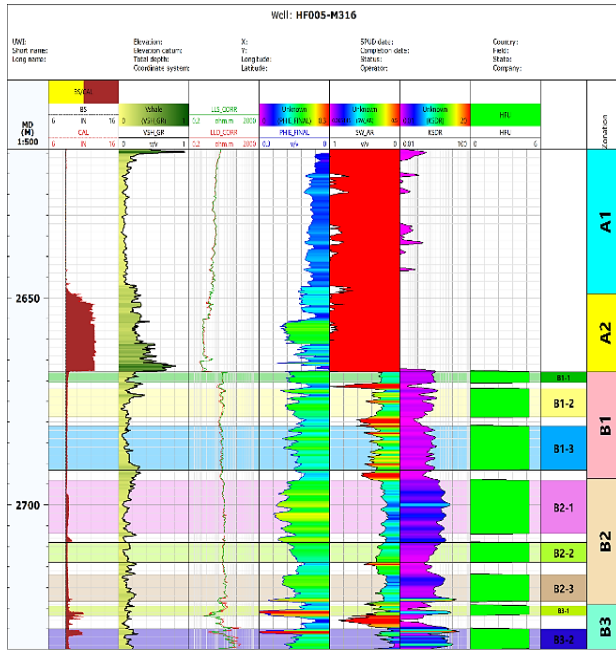
Fig. 13. Flow units in HF005-M316 in Sadi Formation

5- Discussion

Within the oil and gas industry, limestone is one of the most commonly recognized reservoir rocks. [32]. Several approaches can be utilized to determine lithology; one of these approaches relies on well logs, yielding dependable conclusions. For this investigation, (N-D) and (M-N) cross plots were utilized. The (N-D) cross-plot integrates two porosity logs, while the (M-N) cross incorporates three. These plots enable the researcher to assess the effects of gas and secondary porosity and provide a more accurate lithology evaluation. Fig. 2 and Fig. 3 show that the primary lithology of the Sadi Formation in this field is limestone (calcite). This is confirmed by the neutron porosity intersecting with bulk density logs at the limestone line on the Schlumberger lithology chart (N-D). Additionally, secondary porosity was identified, as shown by the movement of data points towards their respective orientations on the (M-N) plot. These findings are further validated by drilling cuttings from wells, which also confirm the presence of limestone. In this study, Gamma ray logs were preferred over other techniques due to their robustness and ability to account for various factors influencing log readings, such as poor density log quality in bad holes. Gamma-ray logs are specifically designed to measure the natural radioactivity of the formation, distinguishing shale (high radioactivity) from limestone (low radioactivity) [33]. According to the findings presented in Fig. 4, the Sadi Formation is a clean formation. This is demonstrated by the fact that the volume of shale computed by GR is somewhat lower than the cut-off value, with the exception of a few meters of shaly limestone.

In porosity estimation, the purpose for utilizing a sonic log in the washout intervals is because of the poor hole condition, which reduces the reading and puts less trust in the density log measurement. As a result, the porosity will

be inaccurate when there is a large washout in the well, as is the case with some intervals in our study. [34], So, porosity was estimated with (N-D) logs for the Sadi reservoir except the interval with large washout, which was calculated with a sonic log. The final estimated porosity was validated by core porosity, which shows the highest porosity in unit B2, which that found to is the best unit in the Formation as seen in Fig. 5.

Archie's equation used to predict the water saturation based on the resistivity log in a distinct formation (heterogeneous and clean homogeneous formations), the accuracy of the Archie equation depends on the preciseness of the basic input parameter: Rt, Rw, Ø, Thus the first issue in reliably computing water saturation from resistivity logs was identifying adequate values for Archie's parameters (a, m, and n), which change based on rock lithology and porosity. (a, m, n) determined by Pickett plot, the calculated water saturation is validated with core water saturation as seen in Fig. 6 good matching between log and core water saturation.

Because the porosity-permeability relationship of core data to construct an equation to predict permeability has a poor R^2 due to its heterogeneity, the second alternative was immediately applied by using the flow zone indicator (FZI) approach. This was done for permeability. The existence of four flow units is demonstrated in Fig. 7. Samples with the same FZI value tend to have similar characteristics of the pore throat, and as a result, they belong to the same flow unit. As a result, the data on porosity and permeability were categorized according to the FZI values, as demonstrated in Fig. 8. Equations in Table 1 was generated for each flow unit used with the porosity to estimate permeability for the unit of interest. Fig. 9 shows the predicted permeability by the FZI approach, which is validated with core permeability.

According to the analysis hydrocarbons accumulated in the lower section of Sadi formation (B1, B2, B3), Fig. 11 illustrates that B2 unit with highest porosity, lowest water saturation, low shale volume and good permeability is the best unit in Sadi Formation which contribute with (20.1 m). Well log interpretation techniques were used to determine the flow unit of the formation, which was based mainly on the variation in porosity and water saturation, where eight flow units were recognized in the Sadi Formation, three flow units determined within each zone (B1, B2) and the other two flow units within zone B3.

6- Conclusions

This study identified the primary flow units of the Sadi Formation within sections B1, B2, and B3, with section B2 being the most productive. It has a productive thickness of 20. 1 meter and contains three distinct flow units. Lithological characterization of the Sadi reservoir utilized Neutron-Density and M-N cross-plots analyses, confirming limestone as the most dominant mineral in the reservoir's formation. This finding is further confirmed by cutting analysis, which revealed that water zone A is separated from the hydrocarbon zone (B) by thin layers of shaly limestone.

The Shale volume in the Sadi Formation, mainly composed of limestone, was determined to be less in volume based on gamma ray logs, which were identified as the most reliable method for estimating shale volume. Effective porosities were obtained from the neutron log, sonic log, and density log. While the neutron-density model was applied to all reservoir units, the sonic model was specifically used under poor hole conditions.

Given the Sadi reservoir's heterogenous limestone nature and low shale content, water saturation was calculated using Archie's equation. Furthermore, permeability was estimated using the FZI method due to the heterogeneous nature of the reservoir's permeability. The results showed mean permeability values of 0.48 md for B1, 3.4 md for B2 and 0.27 md for B3.

Through well log interpretation techniques, eight different flow units were identified within the formation: three in B1, three in the B2 and two in B3 zones.

References

[1] G. B. Asquith, D. Krygowski, and C. R. Gibson, *Basic well log analysis*, 2nd Edition: AAPG Methods in Exploration Series 16. Oklahoma: American Association of Petroleum Geologists Tulsa, 2004, pp. 244.

[2] T. Ahmed, *Working guide to reservoir rock properties and fluid flow*, 1st ed. USA: Gulf Professional Publishing, 2009, pp. 261.

[3] R. M. Idan, A. L. Salih, O. N. Al-Khazraji, and M. H. Khudhair, "Depositional environments, facies distribution, and porosity analysis of Yamama Formation in majnoon oilfield. Sequence stratigraphic approach," *The Iraqi Geological Journal.*, pp. 38–52, 2020, https://doi.org/10.46717/igj.53.1D.4Rw-2020-05-03

[4] H. Liu, *Principles and Applications of Well Logging*, 1st ed. in Springer Mineralogy. Berlin, Heidelberg: Springer Berlin Heidelberg, 2017, https://doi.org/10.1007/978-3-662-53383-3

[5] A. Poupon and R. Gaymard, "The evaluation of clay content from logs," in *SPWLA Annual Logging Symposium*, SPWLA, 1970, pp. 546–547.

[6] R. J. Jenkins, "Accuracy of porosity determinations," *The Log Analyst*, vol. 7, Mar. 1996.

[7] S. Cannon, *Petrophysics: a practical guide*, 1st ed. UK: John Wiley & Sons, 2015, https://doi.org/10.1002/9781119117636.ch10

[8] U. Ahmed, S. F. Crary, and G. R. Coates, "Permeability estimation: the various sources and their interrelationships," *Journal of Petroleum Technology*, vol. 43, pp. 578–587, May 1991, https://doi.org/10.2118/19604-PA

[9] J. O. Amaefule, M. Altunbay, D. Tiab, D. G. Kersey, and D. K. Keelan, "Enhanced reservoir description: using core and log data to identify hydraulic (flow) units and predict permeability in uncored intervals/wells," in *SPE Annual Technical Conference and Exhibition*, SPE, Oct. 1993, pp. 205–220, https://doi.org/10.2118/26436-MS

[10] R. A. Hashim and G. M. Farman, "Evaluating Petrophysical Properties of Sa'di Reservoir in Halfaya Oil Field," *The Iraqi Geological Journal*, vol. 56, pp. 118–126, Oct. 2023, https://doi.org/10.46717/igj.56.2D.9ms-2023-10-15

[11] B. A. Al-Baldawi, "Evaluation of petrophysical properties using well logs of yamama Formation in abu amood oil field, southern Iraq," *The Iraqi Geological Journal*, vol. 54, pp. 67–77, May 2021, https://doi.org/10.46717/igj.54.1E.6Ms-2021-05-27

[12] J. Dewan, *Essentials of modern open-hole log interpretation*. USA: PennWell Books, Tulsa, 1983.

[13] U. Alameedy, G. M. Farman, and H. Al-Tamemi, "Mineral Inversion Approach to Improve Ahdeb Oil Field's Mineral Classification," *The Iraqi Geological Journal*, vol. 56, pp. 102–113, Aug. 2023, https://doi.org/10.46717/igj.56.2B.8ms-2023-8-17

[14] R. A. Hashim and G. M. Farman, "How to Estimate the Major Petrophysical Properties: A Review," *Iraqi Journal of Oil & Gas Research*, vol. 3, pp. 43–58, Apr. 2023, https://doi.org/10.55699/ijogr.2023.0301.1037

[15] A. H. Tali and G. M. Farman, "Use conventional and statistical methods for porosity estimating in carbonate reservoir in southern iraq, case study," *The Iraqi Geological Journal*, vol. 54, pp. 30–38, Oct. 2021. https://doi.org/10.46717/igj.54.2D.3Ms-2021-10-22

[16] A. Buono, S. Fullmer, K. Luck, K. Peterson, H. king, and P. J. More, "Quantitative digital petrography: full thin section quantification of pore space and grains," in *SPE Middle East Oil and Gas Show and Conference*, SPE, Mar. 2019. https://doi.org/10.2118/194899-MS

[17] V. Krutko, B. Belozerov, S. Budennyy, E. Sadikhov, and O. Kuzmina, "A new approach to clastic rocks pore-scale topology reconstruction based on automatic thin-section images and CT scans analysis," in *SPE Annual Technical Conference and Exhibition*, SPE, Oct. 2019. https://doi.org/10.2118/196183-MS

[18] M. Abedini, M. Ziaii, and J. Ghiasi-Freez, "The application of Committee machine with particle swarm optimization to the assessment of permeability based on thin section image analysis," *International Journal of Mining and Geo-Engineering*, vol. 52, pp. 177–185, Dec. 2018.

[19] Y. J. Tawfeeq and J. A. Al-Sudani, "Digital rock samples porosity analysis by OTSU thresholding technique using MATLAB," *Iraqi Journal of Chemical and Petroleum Engineering*, vol. 21, pp. 57–66, Sep. 2020. https://doi.org/10.31699/IJCPE.2020.3.8

[20] J. Ghiasi-Freez, I. Soleimanpour, A. Kadkhodaie-Ilkhchi, M. Ziaii, M. Sedighi, and A. Hatampour, "Semi-automated porosity identification from thin section images using image analysis and intelligent discriminant classifiers," *Computers & geosciences*, vol. 45, pp. 36–45, Aug. 2012. https://doi.org/10.1016/j.cageo.2012.03.006

[21] G. L. Bowers and T. J. Katsube, "Chapter 5: The Role of Shale Pore Structure on the Sensitivity of Wire-Line Logs to Overpressure," in *Pressure Regimes in Sedimentary Basins and Their Prediction*, The American Association of Petroleum Geologists, 2001, pp. 43–60. https://doi.org/10.1306/M76870C5

[22] S.-L. Kung, C. Lewis, and J.-C. Wu, "A technique for improving pseudo-synthetic seismograms generated from neutron logs in gas-saturated clastic rocks," *Journal of Geophysics and Engineering*, vol. 10, p. 035015, Jun. 2013. https://doi.org/10.1088/1742-2132/10/3/035015

[23] I. Taggart, "Effective versus Total Porosity Based Geostatistical Models: Implications for Upscaling and Flow Simulation," *Transport in Porous Media*, vol. 46, pp. 251–268, Feb. 2002. https://doi.org/10.1023/A:1015052712760

[24] M. A. Zainab, I. A. Almallah, and F. M. Al-Najm, "Petrophysical properties evaluation using well logging of the upper sand member of Zubair Formation in Zubair oil Field, Southern Iraq.," *Basrah Journal of Science*, vol. 37, pp. 456–480, 2019.

[25] Z. A. Mahdi and G. M. Farman, "Estimation of Petrophysical Properties for the Zubair Reservoir In Abu-Amood Oil Field," *The Iraqi Geological Journal*, vol. 56, pp. 32–39, Feb. 2023. https://doi.org/10.46717/igj.56.1B.3ms-2023-2-11

[26] L. I. Schlumberger, "Principles and Application: Schlumberger Wireline and Testing," *Houst. Tex.*, pp. 21–89, 1989.

[27] M. Nabih, A. Ghoneimi, A. Essa, and A. H. Saleh, "A new vision for hydrocarbon trapping of Alam El-Bueib Formation in Aman oil field using Fault seal analysis technique, northern Western Desert, Egypt.," *Journal of Petroleum and Mining Engineering*, vol. 24, pp. 53–66, Mar. 2023. https://doi.org/10.21608/JPME.2023.191475.1152

[28] J. A. Al-Sudani, H. K. Mustafa, D. F. Al-Sudani, and H. Falih, "Analytical water saturation model using capacitance-resistance simulation: clean and shaly formations," *Journal of Natural Gas Science and Engineering*, vol. 82, p. 103325, Oct. 2020. https://doi.org/10.1016/j.jngse.2020.103325

[29] W. H. Fertl, "Advances in well logging, well interpretation," *Oil & gas journal*, vol. 82, pp. 85–91, 1984.

[30] S. S. Zughar, A. A. Ramadhan, and A. K. Jaber, "Petrophysical Properties of an Iraqi Carbonate Reservoir Using Well Log Evaluation," *Iraqi Journal of Chemical and Petroleum Engineering*, vol. 21, pp. 53–59, Mar. 2020. https://doi.org/10.31699/IJCPE.2020.1.8

[31] Z. Riazi, "Application of integrated rock typing and flow units identification methods for an Iranian carbonate reservoir," *Journal of petroleum science and engineering*, vol. 160, pp. 483–497, Jan. 2018. https://doi.org/10.1016/j.petrol.2017.10.025

[32] O. Serra, *The Acquisition of Logging Data: Part A*, 1st ed. USA: Elsevier, 1984.

[33] H. Y. Ali, G. M. Farman, and M. H. Hafiz, "Study of petrophysical properties of the Yamama Formation in Siba Oilfield," *The Iraqi Geological Journal*, pp. 39–47, Sep. 2021. https://doi.org/10.46717/igj.54.2C.4Ms-2021-09-23

[34] D. Ellis, "Formation porosity estimation from density logs," *Petrophysics-The SPWLA Journal of Formation Evaluation and Reservoir Description*, vol. 44, pp. 306–316, Sep. 2003.

تقييم الخصائص البتروفيزيائية لتكوين السعدي في حقل الحلفاية النفطي، جنوب العراق

مصطفى محمود هاشم [٢،١]، غانم مديح فرمان [١]، *، احمد عسكر [٣]

١ قسم هندسة النفط، كلية الهندسة، جامعة بغداد، العراق

٢ قسم هندسة النفط، كلية الهندسة، جامعة كربلاء، العراق

٣ قسم الجيوفيزياء، كلية التحسس النائي و الجيوفيزياء، جامعة الكرخ للعلوم، العراق

الخلاصة

يهدف البحث الى تقييم الخواص البتروفيزيائية لمكمن السعدي (تشبع السوائل و النفاذية و المسامية) لتحديد افضل وحدات الجريان ضمن مكمن السعدي. من تفسير بيانات السجل المفتوح لخمسة ابار يتم تحديد الخواص البتروفيزيائية لمكمن السعدي في حقل الحلفاية. اعتمادا على الخواص الناتجة يمكن تقسيم سمك المكمن (120- 130) مترا الى وحدتين رئيسيتين وحدة عليا A ويتراوح سمكها من (45- 50) مترا حيث تكون من الحجر الجيري و الجزء الاسفل منها يحتوي على نسبة عالية من السجيل؛ وحدة سفلى يتراوح سمكها (70-80) مترا وتنقسم الى ثلاث وحدات فرعية (B1,B2,B3) حيث وجدت من الحجر الجيري . نتائج الدراسة تشير الى ان مقاومة الماء للتكوين (Rw=0.04) , و مقاومة راشح الطين (Rmf=0.06) , و تم حساب معاملات ارجي من خلال (Pickett plot), تم قياس الخواص البتروفيزيائية بالاعتماد على سلسلة من العمليات التي تتضمن (تحديد صخارية المكمن, حساب كمية السجيل, حساب المسامية للمكمن, حساب التشبع المائي, حساب النفاذية الصخرية), تم تحديد صخارية المكمن على كونها من الحجر الجيري اعتمادا على مخططات (N-D, M-N). جحم السجيل ضمن مكمن السعدي تم حسابه من خلال اشعة كاما كونها الاكثر دقة في هذا المجال حيث يتراوح حجم السجيل (٧-٥٨) % , تم احتساب قيم المسامية بالاعتماد على مجموعة من المجسات (neutron-density) في الاعماق التي تكون بدون تهدم لجدار البئر و (sonic) في مناطق التهدم. و تشبع الماء مع عمق التكوين باستخدام معادلة ارجي. حيث وجد ان افضل منطقة حاوية على نسبة عالية من المواد الهيدروكاربونية في مكمن السعدي تتركز في الوحدة الثانية حيث تحتوي على اربعة انواع من السحنات الصخرية وذلك باستخدام طريقة (FZI). حيث ان المنطقة المنتجة تكون بسمك (٢٠,١) متر ضمن الوحدة الثانية للمكمن (B). و اخيرا نتيجة لهذه الدراسة تحليل بيانات اللباب و بيانات تسجيل الابار المفتوحة تم تحديد ثمان وحدات للجريان مقسمة الى ثلاث وحدات لكل من المنطقتين (B1, B2) و وحدتان في المنطقة السفلى (B3).

الكلمات الدالة: تكوين السعدي، حقل الحلفاية النفطي، الخواص البتروفيزيائية.